ELSEVIER

Optics & Laser Technology 31 (1999) 85–94

Optics & Laser Technology

www.elsevier.com/locate/optlastec

Laser Doppler anemometry and the acousto-optic effect ☆

R.I. Crickmore [a,*], S.H. Jack [b], D.B. Hann [b], C.A. Greated [b]

[a] *Defence Evaluation and Research Agency, c/o Winfrith Technology Centre Dorchester, Dorset DT2 8XJ, UK*
[b] *The University of Edinburgh, Edinburgh, UK*

Abstract

This paper deals with the effect of phase variations along the paths of the laser beams due to refractive index changes caused by the acousto-optic effect, when an LDA system is used to measure sound waves. Theoretical and experimental results will be discussed. A theoretical expression will be developed for the movement of the fringes in terms of the angle of the sound wave, the wavenumber and the distance of propagation of the laser beams. Results will show that as the wavenumber increases, the angle at which the maximum amplitude of the fringe movement occurs tends away from $\pi/2$ to the laser beam bisector, and towards the angle of the laser beams. It will also be shown that the phase modulations detected experimentally are in reasonable agreement with those predicted theoretically.

1. Introduction

Laser Doppler anemometry is an optical technique which allows single point measurements of the flow rate to be determined. Much work has been carried out in the field of LDA both in the development of the technique and in the analysis of LDA measurements since details of the technique were first published [1]. The principle behind LDA is that two coherent laser beams are brought to a focus at a point where the velocity of a flow is to be determined. When they intersect they create an interference pattern and the particles which are suspended in the flow pass across these fringes, scattering the laser light, Fig. 1. This scattered laser light then contains all the information about the flow and is collected and stored as a Doppler signal. This signal is usually analysed in one of the following ways: spectral analysis [2], frequency tracking [3] or photon correlation [4].

The LDA technique has recently been developed for measuring instantaneous acoustic particle velocities, thus allowing measurements to be made in complex sound fields [5,6]. The techniques of spectral analysis and photon correlation mentioned above are unable to analyse signals of more than one frequency and therefore, in the case of complex sound fields, a recently developed variation of the frequency tracking technique is used [7]. This technique allows an instantaneous measurement of the velocity to be made and enables the frequency, amplitude and instantaneous phase of the various components of the signal to be determined [8].

When a sound wave passes through a medium it produces regions of tension and compression which, due to the acousto optic effect, cause variations in the refractive index. In LDA, when the laser beam passes through these refractive index variations its optical path length changes. When the two laser beams intersect to create interference fringes, the variations in path length result in a moving fringe pattern rather than a stationary one. There are therefore two types of movement which have to be considered when using LDA in sound fields. Firstly, the particles in the fringes oscillate due to the sound wave and secondly, the fringes oscillate due to the varying phase difference in the laser beams. Thus, the modulation of the scattered light collected will be due to the apparent motion of the particles in the fringes, that is the oscillation of

☆ Published with the permission of the Controller of Her Britannic Majesty's Stationary Office.

* Corresponding author.
E-mail address: rcrickmore@dera.gov.uk (R.I. Crickmore)

0030-3992/99/$ - see front matter.
PII: S0030-3992(99)00030-4

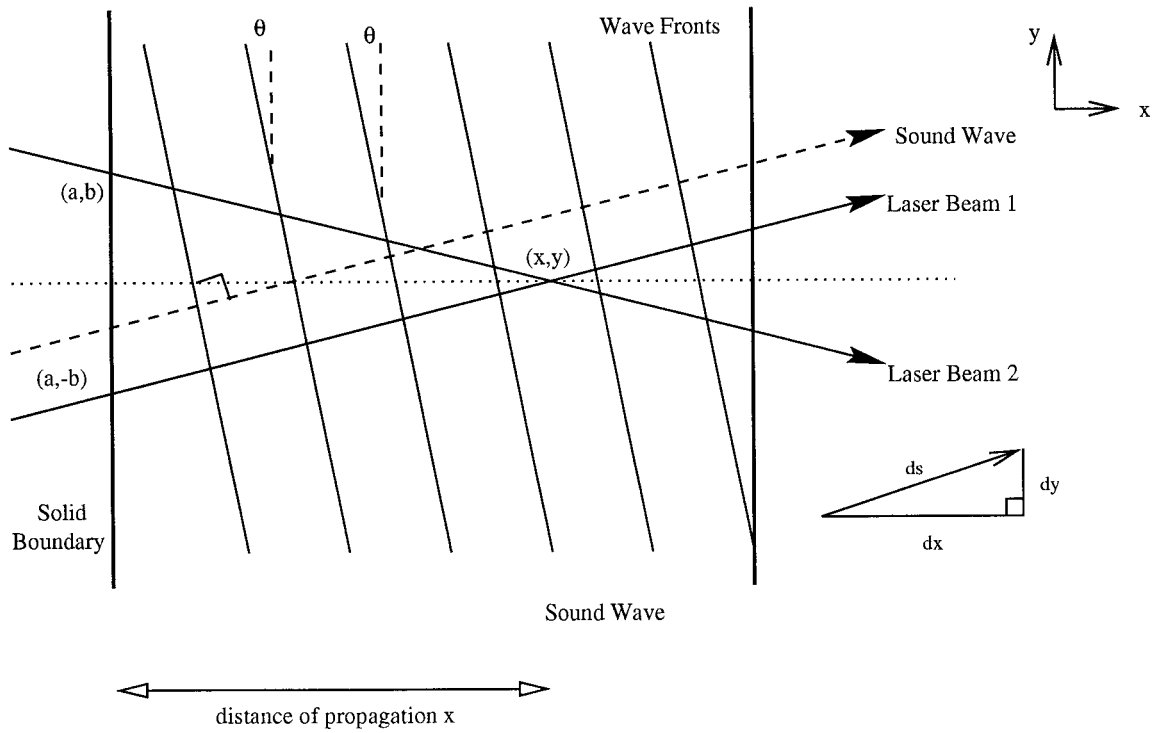

Fig. 1. LDA set-up in sound field.

both the particles and the fringes. If the acousto-optic effect is dominant when the Doppler signal is analysed, the instantaneous frequency determined will be mainly due to the oscillating fringes rather than the oscillating particles and therefore the instantaneous frequencies obtained may not be an accurate representation of the acoustic flow at the point of beam intersection.

Work carried out to date on the use of LDA in sound fields [6,9] has not taken into account this acousto-optic effect due to the fact that the measurements have been made at either short distances of propagation or at low frequencies and in these cases the acousto-optic effect is negligible [10].

2. Path differences in laser beams due to refractive index variations

When the laser beams in the LDA set-up meet, they will have zero path difference and therefore zero phase difference only if their optical path lengths are equal. Therefore, in order to determine the amount of fringe movement, it is necessary to know the path difference, δ, between the two beams

$$\delta = \mathrm{opl1} - \mathrm{opl2}, \tag{1}$$

where opl1 and opl2 are the optical path lengths of the two light beams.

The optical path length of each light beam is given by

$$\mathrm{opl} = \int_c n \, \mathrm{d}s. \tag{2}$$

The two-dimensional refractive index change, n, of the sound wave which affects the light beams is given by

$$n(x,y) = n_{\mathbf{o}} - \Delta n \sin(k_x x + k_y y + \omega t), \tag{3}$$

where n_o is the refractive index of the medium without the presence of a strain field, Δn is the amplitude of the refractive index variations, ω is the angular sound frequency, t is the time and k_x and k_y are the wave-numbers in the x and y directions.

The optical path length of a light beam propagating through a sound wave at an angle to the y-axis can therefore be written as

$$\mathrm{opl} = \int_c \big(n_o - \Delta n \sin\big(k_x x + k_y y + \omega\big)\big)\mathrm{d}s. \tag{4}$$

In this case the contour c is a straight line with equation

$$y - y_2 = m(x - x_2) \tag{5}$$

Therefore, substituting for x, k_x and k_y in Eq. (3) and using

$$\delta s = \sqrt{\big(\delta x^2 + \delta y^2\big)}$$

$$\frac{\delta s}{\delta y} = \sqrt{\left(\frac{\delta x}{\delta y}\right)^2 + 1} \tag{6}$$

from Fig. 1 gives

$$\begin{aligned}\text{opl} = \sqrt{1+\left(\frac{1}{m}\right)^2}\Bigg[& n_o(y_1 - y_2) \\ &+ \frac{m\Delta n}{k\cos\theta + km\sin\theta}\Bigg]\Bigg[\cos\left(\frac{k}{m}\cos\theta(y_1 - y_2 + mx_2)\right. \\ &\left. + ky_1\sin\theta - \omega t\right) - \cos\left(\frac{k}{m}\cos\theta(y_2 - y_2 + mx_2)\right. \\ &\left. + ky_2\sin\theta - \omega t\right)\Bigg].\end{aligned}$$

In this case, beam 1 is integrated from the point $(a,-b)$ to (x, y) and beam 2 is integrated from the point (x, y) to (a, b). The expressions for the optical path length are only integrated over the y variable and due to the relative negative gradient of beam 2, the integral is taken from (x, y) to (a, b) to compensate for the change in the sign of the differential. Therefore the path difference, δ, is

$$\delta = \text{opl1} - \text{opl2}$$

$$\begin{aligned}\delta = &\sqrt{1+\left(\frac{1}{m_1}\right)^2}\left(n_o(-b-y)\right. \\ &\left. + \frac{m_1\Delta n}{k\cos\theta + km_1\sin\theta}\right)\Bigg[\cos\left(\frac{k}{m_1}\cos\theta(m_1 a)\right. \\ &\left. - kb\sin\theta - \omega t\right) - \cos\left(\frac{k}{m_1}\cos\theta(y + b + m_1 a)\right. \\ &\left. + ky\sin\theta - \omega t\right)\Bigg] - \sqrt{\left(\frac{1}{m^2}\right)^2}\left(n_o(y-b)\right. \\ &\left. + \frac{m_2\Delta n_o}{k\cos\theta + km_2\sin\theta}\right)\Bigg[\cos\left(\frac{k}{m_2}\cos\theta(y\right. \\ &\left. - b + m_2 a) + ky\sin\theta - \omega t\right) \\ &- \cos\left(\frac{k}{m_2}\cos\theta(m_2 a) + kb\sin\theta - \omega t\right)\Bigg].\end{aligned} \tag{8}$$

While Eq. (8) can not be solved analytically in terms of y, it can be simplified and then solved. The value of y for which $\delta = 0$ can be found by assuming that any fringe movement in the x direction is negligible so it is possible to set $x = 0$, and the quantity $((y+b)/x)^2$ is small. Using these facts and neglecting all terms with y greater than y' produces

$$y = \frac{\Delta n\big(\cos(kx\cos\theta + ky\sin\theta) - \cos(kb\sin\theta)\big)\big(2x^2 + b^2\big)\sin\theta}{2n_o k(b^2\sin^2\theta - x^2\cos^2\theta) - 2\Delta n\big(\cos(kx\cos\theta + ky\sin\theta) - \cos(kb\sin\theta)\big)x\cos\theta} \tag{9}$$

Since $ky \ll 1$

$$\cos(ky\sin\theta) \approx 1$$

$$\sin(ky\sin\theta) \approx 0$$

and $\Delta n \ll n_o$

$$y = \frac{\Delta n\big(\cos(kx\cos\theta) - \cos(kb\sin\theta)\big)\big(2x^2 + b^2\big)\sin\theta}{2n_o k(b^2\sin^2\theta - x^2\cos^2\theta)} \tag{10}$$

3. Apparent motion of particles in fringes

When LDA is used in sound fields the particles move due to the sound wave, the interference fringes move due to the acousto-optic effect and therefore the apparent position of the particles in the fringes will change with respect to the detector. It is therefore necessary to determine whether the particle movements induced by the sound wave are in or out of phase with the motion of the fringes due to the acousto-optic effect and also to determine the magnitude of the acousto-optic effect, y_{amp}, on the Doppler signal.

It has been shown [11] that

$$\Delta n = 1.63 \times 10^{-10}\Delta P, \tag{11}$$

where ΔP is the amplitude of the acoustic pressure.

The amplitude of the acoustic velocity is related to the acoustic pressure by

$$\Delta U = \frac{\Delta P}{\rho v}, \tag{12}$$

where ρ is the density of the medium and v is the sound velocity.

It is known that the acoustic velocity $\Delta U = 2\pi A_m f$, where A_m is the amplitude of the acoustic wave and f is the sound frequency, therefore for water parameters

$$\Delta n = 0.367 A_m k \tag{13}$$

and

$$y = 0.367\frac{A_m\big(\cos(kx\cos\theta) - \cos(kb\sin\theta)\big)\big(2x^2 + b^2\big)\sin\theta}{2n_o(b^2\sin^2\theta - x^2\cos^2\theta)}. \tag{14}$$

It is also important to determine whether the two motions are in or out of phase with each other. The form of the refractive index change is

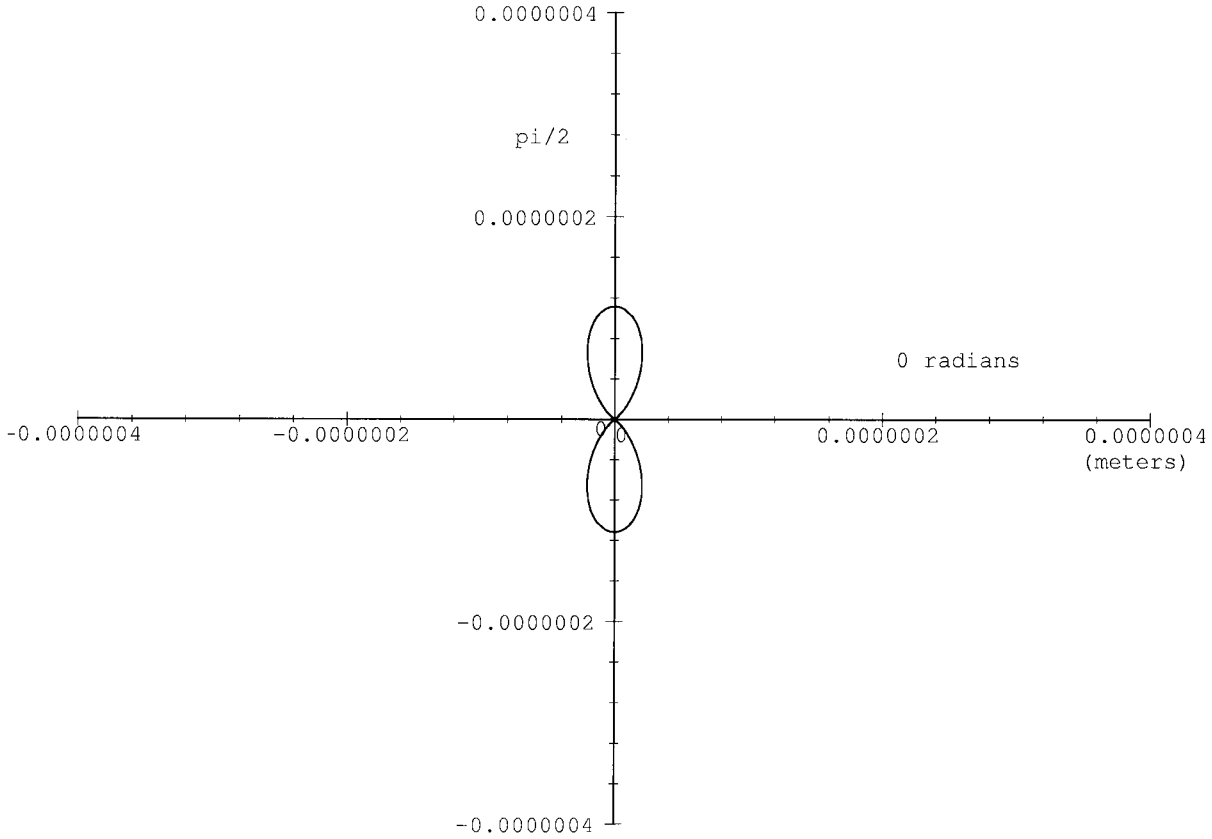

Fig. 2. Polar plot for $k = 15\ \mathrm{m}^{-1}$.

$$n = n_o - \Delta n \cos\left(k_x x + k_y y + k_z z + \omega t\right). \tag{15}$$

It is known that the refractive index variation is proportional to the pressure change from Eq. (11)

$$P \propto \Delta P \sin\left(k_x x + k_y y + k_z z + \omega t\right) \tag{16}$$

and the pressure change is proportional to the acoustic velocity (Eq. (12))

$$U \propto \Delta U \sin\left(k_x x + k_y y + k_z z + \omega t\right). \tag{17}$$

Acoustic velocity is related to the acoustic amplitude thus

$$A \propto A_m \omega \cos\left(k_x x + k_y y + k_z z + \omega t\right). \tag{18}$$

From this it can be said that

$$y \propto \Delta n \propto \Delta p \propto \Delta v \propto A$$

and the motion of the fringes, y, with amplitude y_{amp}, is $\pi/2$ out of phase with the motion of the acoustic wave, A, with amplitude A_m.

Therefore the apparent motion of the particle has the form

$$y(X) = A_m \cos(X) + y_{\mathrm{amp}} \sin(X) \tag{19}$$

Using Eqs. (10) and (13) the form of $y_{\mathrm{amp}}/A_{\mathrm{m}}$ can be determined

$$\frac{y_{\mathrm{amp}}}{A_m} = 0.367 \frac{\left(\cos(kx\cos\theta) - \cos(kb\sin\theta)\right)\left(2x^2 + b^2\right)\sin\theta}{2n_o(b^2\sin^2\theta - x^2\cos^2\theta)} \tag{20}$$

and thus the ratio of the apparent motion to the actual motion of the particles in the fringes has the form

$$\frac{y(X)}{A_m} = \cos(X) + 0.367 \frac{\left(\cos(kx\cos\theta) - \cos(kb\sin\theta)\right)\left(2x^2 + b^2\right)\sin\theta}{2n_o(b^2\sin^2\theta - x^2\cos^2\theta)} \sin(X) \tag{21}$$

for an angle of $\theta = \pi/2$ and for a low wavenumber this reduces to the approximation [10]

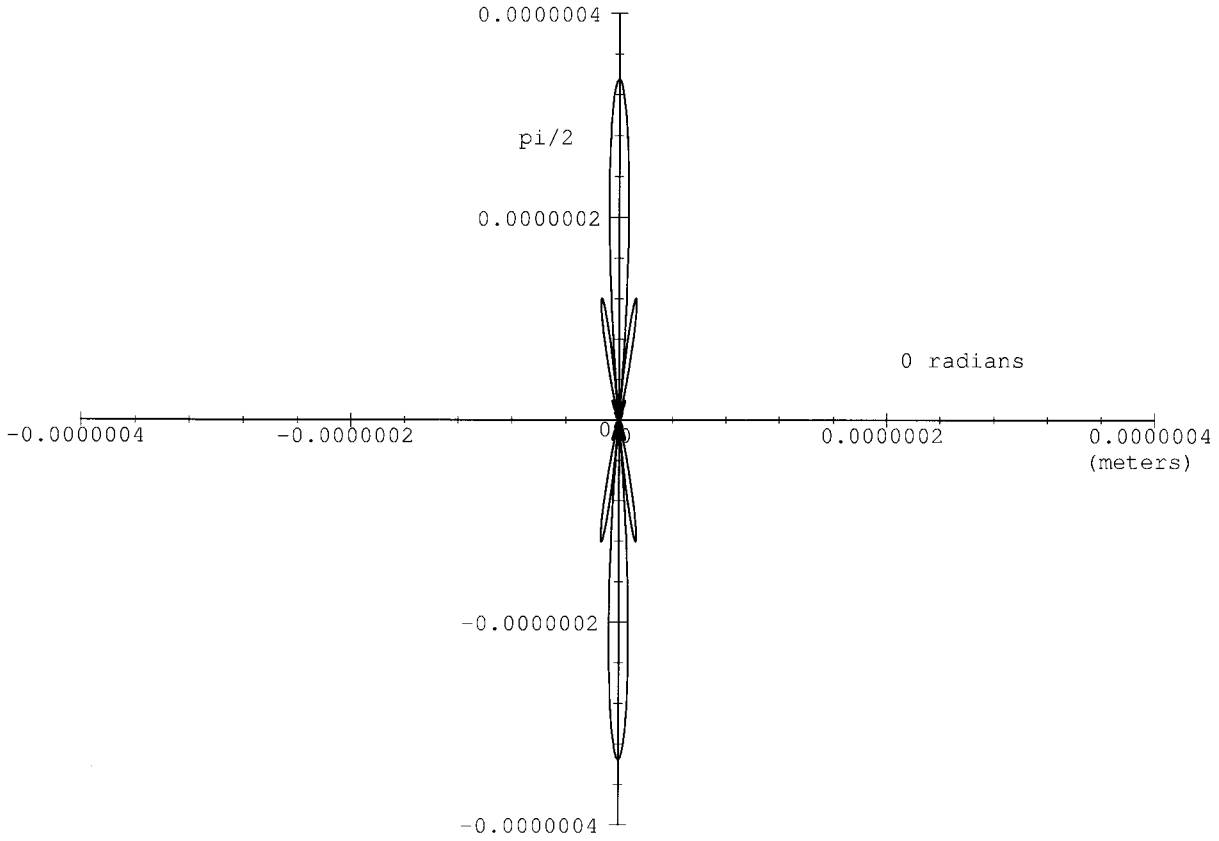

Fig. 3. Polar plot for $k = 100\ \mathrm{m}^{-1}$.

$$\frac{y(X)}{A_m} = \cos(X) + 0.138k^2x^2\sin(X). \tag{22}$$

4. Theoretical results

Using Eq. (10) it is possible to determine the variation of the fringe movement y with angle θ for low, medium and high values of the wavenumber, k. These are shown in Figs. 2–4 and are created for a propagation distance of $x = 0.497$ m and an initial beam separation of 0.06 m ($b = 0.03$ m). In the polar plots, the positive horizontal axis corresponds to an angle of zero radians and the positive vertical axis to an angle of $\pi/2$. It has been shown [10] that for low wavenumbers there is a linear relationship between y and k of the form

$$\frac{y}{\Delta n} = 0.376kx^2 \tag{23}$$

and that the value of y_{amp} always occurs at an angle of $\pi/2$ from the y direction, Fig. 2. As the value of the wavenumber increases, Figs. 3 and 4, this linear relationship no longer holds and the angle at which y_{amp} occurs begins to change.

It can be seen in Fig. 3 that although y_{amp} still occurs at an angle of $\theta = \pm\pi/2$, there are additional angles at which it is possible to obtain a value for y_{amp}. As the wavenumber increases further, Fig. 4, the value of y_{amp} at an angle of $\theta = \pm\pi/2$ decreases and the side peaks have increasing magnitude. The angle of these side peaks corresponds to the angle of the laser beams. This can be understood by looking at Fig. 5.

When the wavenumber is low and the sound wave is propagating parallel to the optic axis, the refractive index changes in both beams are the same and thus there is no path difference whereas when the sound wave is at an angle of $\pi/2$ from the laser beams they are affected to differing degrees and the path difference is a maximum. As the wavenumber increases, an angle of $\pi/2$ creates similar changes in each beam and therefore the path difference is minimal. When the sound wave is at the same angle as the laser beam, one beam will have approximately zero change as all the individual changes cancel each other out and the other beam will have a maximum change, resulting in a maximum path difference between the beams.

5. Experimental details

An experiment using a LDA system to measure

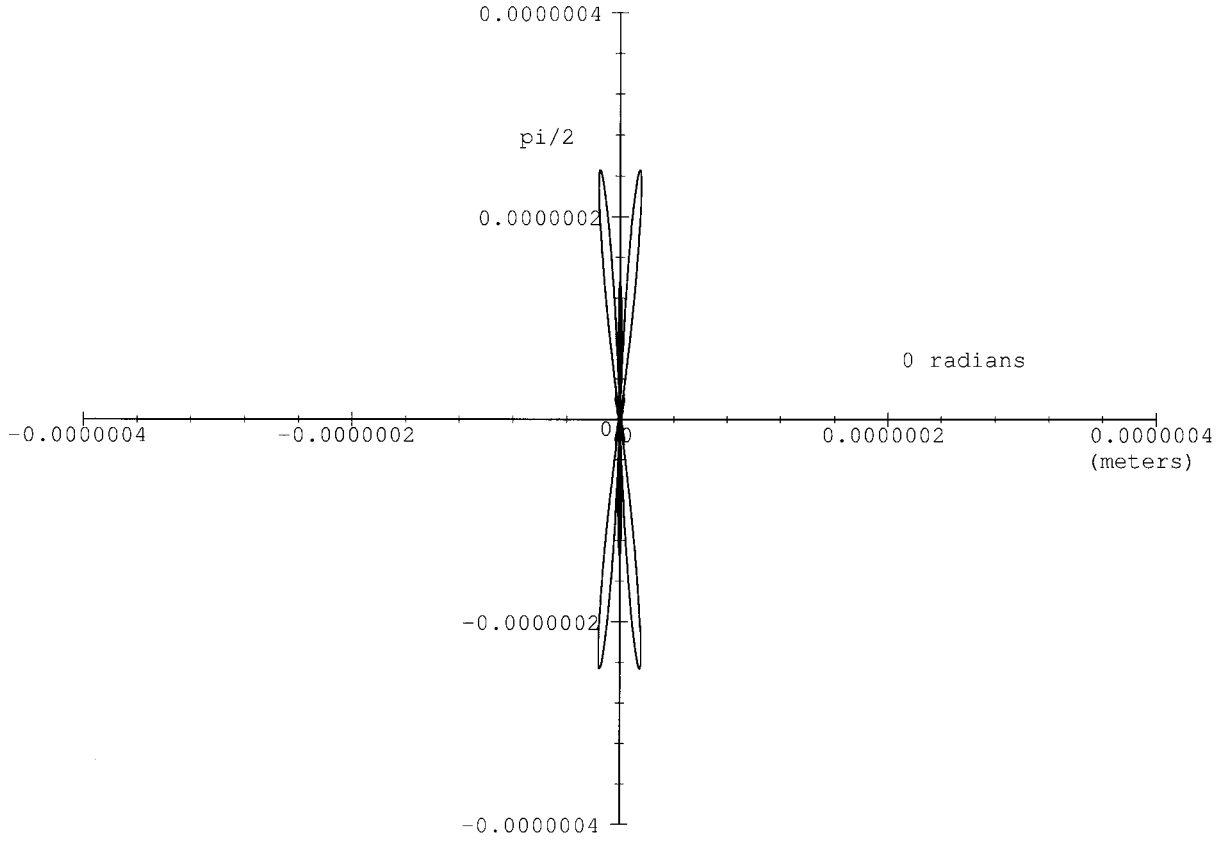

Fig. 4. Polar plot for $k = 150\ \mathrm{m}^{-1}$.

sound was designed so that the acousto-optic modulation would dominate the particle vibration. This was achieved by using a long (50 cm) path length through the water and acoustic frequencies in the range 9–20 kHz. The experiments were carried out in the sonar test tank at DERA Winfrith which is 10 m long, 5 m wide and 5 m deep and has an acoustic antireflection lining on its walls and bottom.

Rather than building all the equipment into a waterproof housing that could be submersed into the tank it was decided that it was simpler to leave the laser and photodetector in air and transmit the light down to an underwater optics unit using fibre optic cables. The underwater part of the system was commercially available equipment intended for use as part of a laser Doppler velocimetry system for measuring fluid flows.

The light source used was a 50 mW frequency doubled, Nd YAG laser which emitted at 532 nm. The laser beam was split using a beamsplitter and each of the two resulting beams were passed through a Bragg cell before being coupled into optical fibres leading to the underwater unit. One Bragg cell had a driving frequency of 80 MHz, while the other was driven at 80.1 MHz. This resulted in the two beams having a frequency difference of 100 kHz, and so light being scattered from a stationary particle without an acoustic wave being present would have a modulation of 100 kHz. The 100 kHz signal acts as a carrier for the acoustic information.

The underwater optics unit forms a beam from each of the fibres, which are initially separated by 60 mm and cross in the water 497 mm away from the unit. At their crossing point the beams are focused to a waist 240 mm in diameter. Light scattered by suspended particles where the beams cross is focused by a lens in the optics unit into a multimode fibre which transmits the light back to the surface. All three optical fibres are enclosed in a waterproof armoured cable.

The light from the return fibre was focused onto a avalanche photodiode (APD) module which consists of an APD with an internal gain of 50, and a current to voltage converter. The output from the APD module was digitised using an analogue to digital converter (ADC) sampling with 12 bit resolution at 500 kHz. The APD signal was input directly into one channel of the ADC and also into another channel having passed through an electronic amplifier and a filter with a passband of 20–180 kHz. The system was set to capture data if the amplitude of the filtered signal exceeded a certain level.

Fig. 6 shows a diagram of the equipment deployed in the sonar tank. Although the intention of these ex-

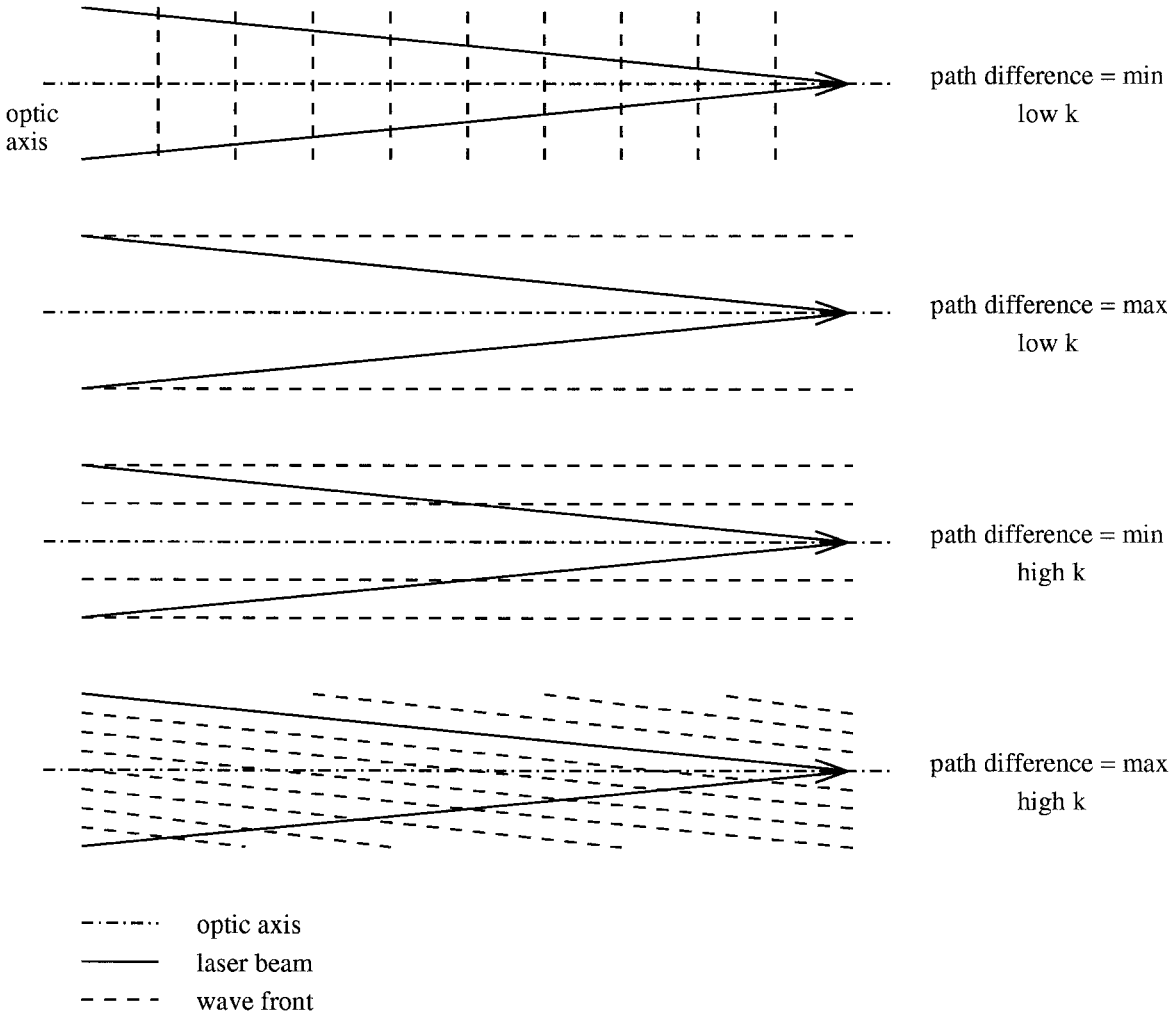

Fig. 5. Variation of path difference with wavenumber and angle of wavefront.

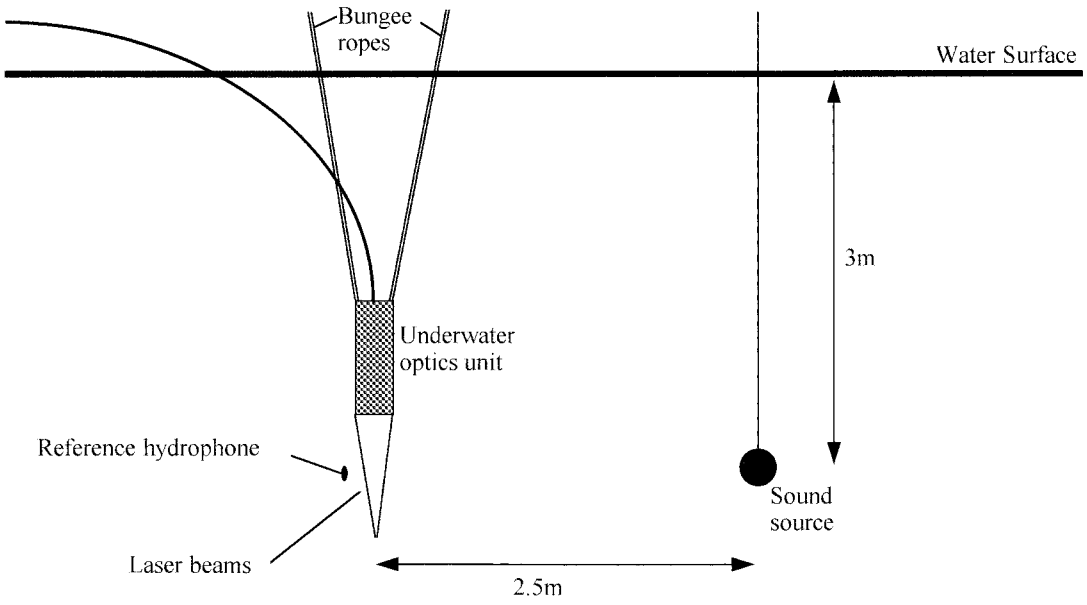

Fig. 6. Experimental arrangement.

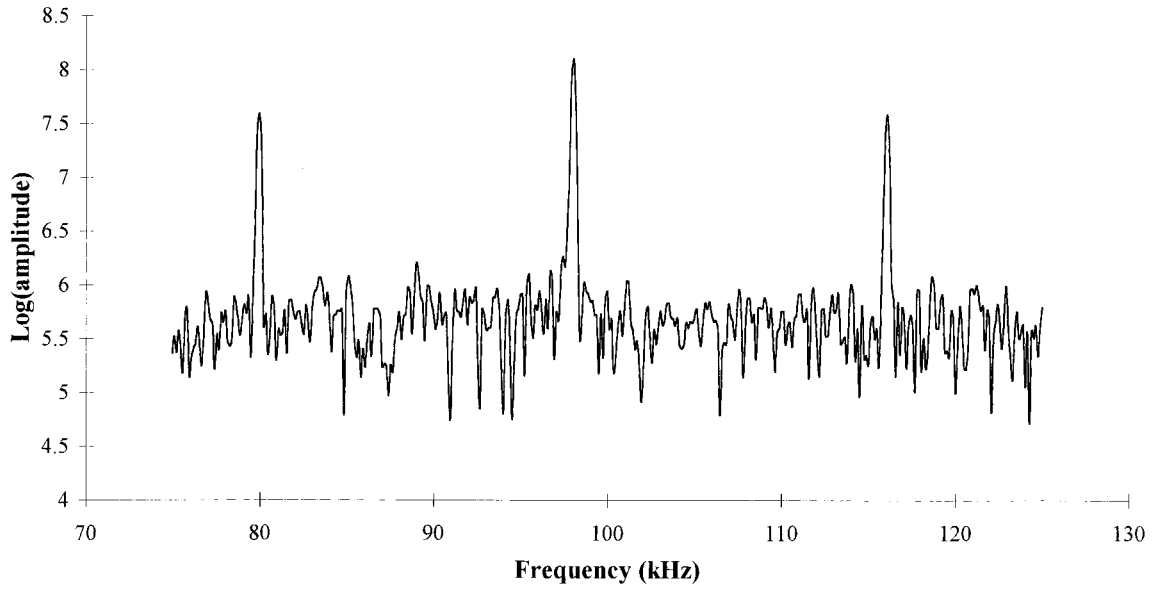

Fig. 7. Spectrum for 18 kHz signal.

periments was to measure the sound by the change in refractive index of the water, the system was still sensitive to any relative motion between the optics head and the water. In particular any vibration coupled to the optics head through its mounting system would appear as a signal. To prevent this from happening the optics unit was suspended underwater using two lengths of elastic bungee ropes which acted as a vibration isolation system.

We used a 15-cm diameter ball projector as the sound source which was suspended so that its centre was at the same depth (~3 m) as the midpoint of the laser beams and separated horizontally from them by 2.5 m. Experiments were carried out using a range of frequencies between 9 and 20 kHz and for a range of pressures. The separation between the sound source and laser hydrophone was sufficient to ensure that the curvature of the acoustic wave over the region travelled by the laser beams was always a small fraction of an acoustic wavelength, and so the wave was a reasonable approximation to a plane wave. To provide an independent measure of the acoustic pressure a conventional reference hydrophone was suspended 25 cm (that is half way to the beam crossing point) underneath the optics unit.

Measurements were made using both pulsed and

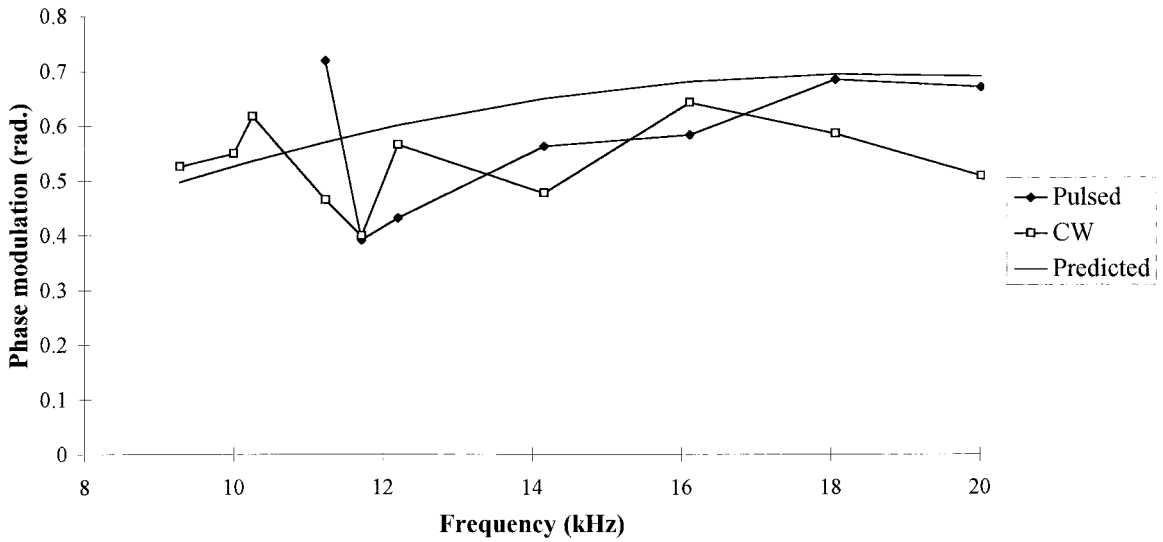

Fig. 8. Variation of phase modulation with frequency.

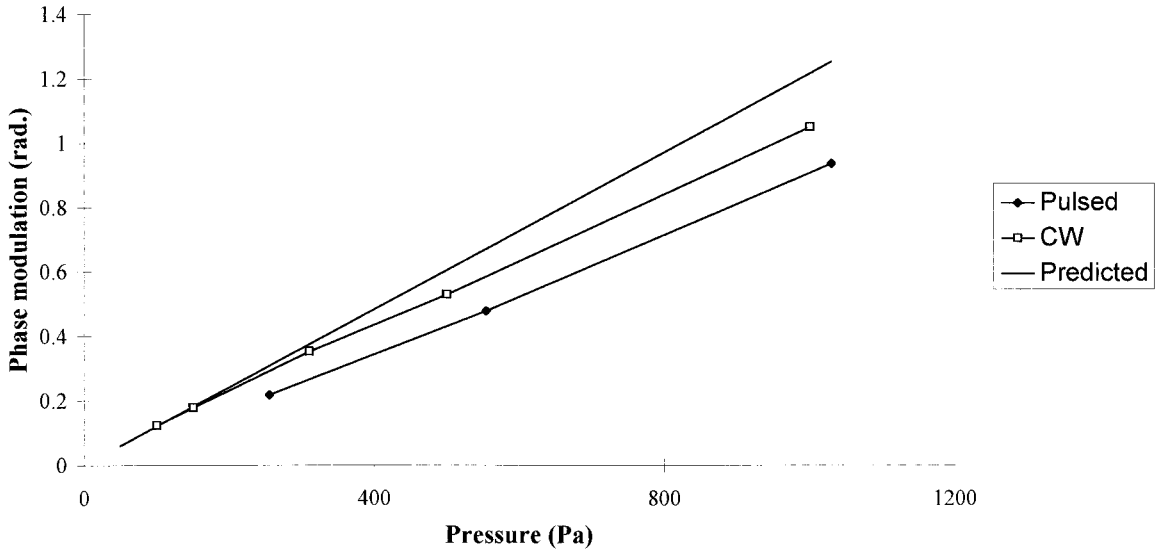

Fig. 9. Variation of phase modulation with pressure.

CW acoustic transmissions. For pulsed transmissions a 2.5-ms pulse was used in order to prevent interference between the direct transmission and the reflection from the water surface. In addition the direct signal from the APD module to the ADC was replaced by the signal from the reference hydrophone. The ADC was triggered to capture data only if there was a significant signal from the APD at 100 kHz, indicating a particle was present in the scattering volume, and a signal from the reference hydrophone indicating that an acoustic signal was present.

6. Data analysis

The data for each particle was analysed to determine the length of time for which a carrier signal at 100 kHz was clearly visible and then an FFT was then carried out on that section of data. It can be shown that the spectrum consists of the carrier peak at 100 kHz and a series of side peaks on either side separated by the acoustic frequency [2]. Fig. 7 shows a spectrum obtained using an acoustic signal at 18 kHz. The optical phase modulation induced between the two laser beams (m) can be determined from the ratio (R) between the amplitudes of the carrier peak and the first side peaks using the equation,

$$R = J_0(m)/J_1(m), \tag{24}$$

where $J_n(\,)$ is the Bessel function of order n.

The phase modulation due to the motion of the fringes predicted using the equations in Sections 2 and 3, was also calculated for each particle using the pressure measured by the reference hydrophone.

7. Experimental results

Fig. 8 shows the values of optical phase modulation measured by the laser hydrophone and those predicted from the pressure measured by the reference hydrophone for an acoustic wave of 500 Pa over a range of frequencies, with either CW or pulsed acoustic transmissions. The measured values are generally within 25% of the predicted values. The differences are probably due to the fact that the acoustic field was not exactly uniform and the laser hydrophone measures a pressure integrated over a distance of 50 cm while the reference hydrophone is only 1 cm long.

Fig. 9 shows the variation of optical phase modulation with acoustic pressure for a frequency of 12 kHz. As predicted there is a linear increase in modulation with pressure for both CW and pulsed acoustic transmissions.

As discussed in Section 4 the phase modulations will be due to a combination of particle vibration and the acousto-optic effect. For the acoustic frequencies and optical arrangement used in these experiments the modulation due to the acousto-optic effect was much greater than that due to particle vibration. For example the particle motion due to a 500-Pa signal at 12 kHz would give a phase modulation of 0.0081 which is a factor of 75 less than the acousto-optic effect. It is therefore clear that the phase modulations being observed are due to the acousto-optic effect rather than particle vibration.

8. Conclusions

When an LDA system is used to measure sound in

water both the motion of the scattering particles and variations in the refractive index due to the acousto-optic effect give rise to a signal, with the signals from the two effects being $\pi/2$ out of phase. The signal due to particle vibration will dominate at lower frequencies and short optical paths lengths through the water, while the acousto-optic effect will become dominant for longer path lengths and higher frequencies. An experiment using an LDA system to measure sound was carried out in which the acousto-optic effect was predicted to produce the largest signal. The phase modulations detected were in reasonable agreement with those predicted by the theory.

References

[1] Yeh Y, Cummins HZ. Localised fluid flow measurements with a He–Ne laser spectrometer. Appl Phys Lett 1964;4:176–8.

[2] Taylor KJ. Absolute calibration of microphones by a laser Doppler technique. J Acoust Soc Am 1981;70(3):393.

[3] Fridman JD, Huffaker RM, Kinnard RF. Laser–Doppler system measures three-dimensional velocity vector and turbulence. Laser Focus 1968;4:34.

[4] Sharpe JP, Greated CA. The measurement of periodic acoustic fields using photon correlation spectroscopy. J Phys D: Appl Phys 1987;20:418–23.

[5] Hann DB, Jack SH, Greated CA, Rinkevichius BS, Greckikhin VA, Tolkachev AV, Stephanov AV. Laser Doppler measurements in complex sound fields. In: LAAA Proc. 7th International Conference, 1997. p. 107–14.

[6] Jack SH, Crickmore RI, Hann DB, Greated CA, Rinkevichius RS. Laser Doppler systems for underwater sounds measurement. A new journal of the Institute of Physics, submitted for publication, 1997.

[7] Grechikhin VA, Rinkevichius BS. Digital Hilbert transform for processing of laser Doppler vibrometry signals. Second International Conference on Vibration Measurements by Laser Technology, Ancona, Italy, 1996.

[8] Hann DB, Greated CA. The measurement of sound fields using laser Doppler anemometry. Acta Acustica, submitted for publication, 1997.

[9] Haunch S. In: A treatise on acoustic radiation, vol. II. Washington, DC: Naval Research Lab, 1983. p. 377 (ch 6).

[10] Jack SH, Hann DB, Greated CA. The influence of the acousto-optic effect on laser Doppler anemometry signals. Rev Sci Instr 1998;69(12):4074–81.

[11] Minnow DA. Guide-lines for the selection of acousto-optic materials. IEEE J Quantum Electron QE 1970;6(4):223–38.